STRUCTURAL AND MAGNETIC PROPERTIES OF MG DOPED CU-ZN FERRITE NANOPARTICLES SYNTHESIZED WITH GREEN TEA EXTRACT

Ravi S. Kawale[1*]

ABSTRACT

The study successfully synthesized Mg-doped Cu-Zn ferrite nanoparticles using a green and eco-friendly method, using green tea extract as a reducing and capping agent. The structural and magnetic properties of the nanoparticles were thoroughly examined using various analytical techniques. X-ray diffraction (XRD) confirmed the formation of a single-phase cubic spinel structure, with an average size of 18 nm. Fourier-transform infrared spectroscopy (FTIR) identified characteristic peaks at 400 cm-1 and 600 cm-1, which correspond to the stretching vibrations of metal-oxygen (M-O) bonds. Scanning electron microscopy with energy-dispersive X-ray spectroscopy (SEM-EDS) showed a consistent spherical shape with an average size of 25 nm. The magnetic properties were significantly influenced by Mg doping, with saturation magnetization (Ms) increasing from 42.5 emu/g for undoped samples to 54.2 emu/g for Mg-doped samples. The coercivity (Hc) values showed a slight decrease, indicating enhanced magnetic stability. The study highlights the wide range of technological domains where these nanoparticles can be applied, taking advantage of their magnetic properties and environmental friendly synthesis.

Keywords: Ferrites, Green tea extract, XRD, FT-IR, SEM-EDS, VSM Analysis

[1*]Department Of Electronics, D.S.M. College, Jintur, Dist. Parbhani- 431509, (MS) India.
Email: ravi.kawale1972@gmail.com

*Corresponding Author: Ravi S. Kawale
*Department Of Electronics, D.S.M. College, Jintur, Dist. Parbhani- 431509, (MS) India.
Email: ravi.kawale1972@gmail.com

Eur. Chem. Bull. **2022**, *11(Regular Issue 12)*, 3551 –3557

3551

1. Introduction:

In recent times, there has been an increasing focus on environmentally friendly and sustainable methods for synthesizing nanomaterials, with the intention of mitigating the environmental issues that are linked to traditional synthesis techniques. In their recent publication, Tamboli et al. (2023) thoroughly examined the current advancements in the synthesis of nanocobalt ferrites and their composites[1]. Their focus was on the use of sustainable resources for environmentally friendly synthesis methods. Their findings highlight the benefits of using environmentally friendly synthesis methods instead of conventional approaches. In this instance, a wide range of natural resources have been investigated for their potential in green synthesis. One notable example is the utilization of pomegranate peel extracts, as highlighted in a study conducted by Huang et al. (2023). Their study highlights the utilization of pomegranate peel waste in the eco-friendly production of Cu/Fe nanoparticles[2]. This research demonstrates the potential of these nanoparticles in effectively removing tetrabromobisphenol A (TBBPA) from water solutions.

In a recent publication by Mousavi et al. (2023), they have presented novel techniques for the synthesis of N-substituted pyrrole derivatives. These methods involve the use of NiFeO anchored to modified carbon hollow microspheres, resulting in a one-pot synthesis approach. The study highlights the recoverable and catalytic properties of the synthesized catalyst in the formation of N-substituted pyrrole derivatives. In a recent study, León-Flores et al. (2023) put forward an innovative approach to enhance the molten salts process[3]. Their proposed methodology, referred to as the 'shocking thermal treatment,' aims to enable the rapid and scalable synthesis of pure phase nickel ferrite nanoparticles with minimal environmental impact. Their findings, backed by XRD and electron microscopy analysis, validate the successful formation of nanostructures. Another significant study is conducted by Iqbal et al. (2023), where they emphasize the environmentally friendly production of nickel-doped magnesium ferrite nanoparticles through combustion[4]. Their research explores the potential applications of these nanoparticles in microwave-assisted optical and photocatalytic processes. The study highlights the structural and morphological characteristics of the synthesized nanoparticles, showcasing spinel cubic structures with a distinctive nano flakes-like shape.

The wide range of methods used in eco-friendly synthesis goes beyond the use of ferrite nanoparticles. Ayyıldız et al. (2023) conducted a study where they utilized a magnetic sorbent to extract lead ions from rooibos tea samples, highlighting the adaptability of green techniques in different fields[5]. This study investigates the green synthesis of Mg-doped Cu-Zn ferrite nanoparticles using green tea extract. It aims to contribute to the growing understanding of sustainable synthesis methods and their potential applications in advanced materials.

2. Material and Methods:

In this study, $Zn_{0.4}Cu_{0.6}Mg_xFe_2O_4$ nanoparticles, with varying Mg content (x = 0, 0.2, 0.4, 0.6), were synthesized through a green and sustainable approach using green tea extract. Metal nitrate solutions, comprising zinc, copper, iron, and magnesium, were meticulously prepared, and the co-precipitation of these solutions was achieved through the addition of sodium hydroxide. Throughout the nanoparticle synthesis process, green tea extract obtained by steeping green tea leaves played a crucial role, serving both as a reducing agent for the nanoparticles and as a protective layer. This method ensures a cost-effective and environmentally friendly synthesis process.

The resulting precipitate underwent maturation, followed by a thorough rinsing process and subsequent re-suspension in ethylene glycol. To enhance the stability of the precipitate, polyvinylpyrrolidone (PVP) was introduced. The solution was then subjected to heating to facilitate the formation of nanoparticles composed of $Zn_{0.4}Cu_{0.6}Mg_xFe_2O_4$. The nanoparticles obtained from this process underwent a series of subsequent washing and drying operations to yield the final product. This synthesis approach not only ensures the tailored composition of the nanoparticles but also emphasizes the use of green tea extract as a versatile and sustainable agent in nanoparticle fabrication[6].

3. Result and Discussion
3.1 XRD Analysis

X-ray diffraction (XRD) analysis was conducted to investigate the crystal structure and phase composition of the synthesized ferrite nanoparticles with varying aluminum content. The XRD patterns were obtained using a high-resolution X-ray diffractometer operating at a wavelength of λ = 1.5406 Å. The XRD patterns of the synthesized nanoparticles were analyzed to determine the crystal structure and lattice parameters.

The XRD analysis aimed to unravel the structural characteristics of $Zn_{0.4}Cu_{0.6}Mg_xFe_2O_4$

Eur. Chem. Bull. **2022**, *11(Regular Issue 12), 3551 –3557*

3552

nanoparticles across varying Mg content (x = 0, 0.2, 0.4, 0.6). The XRD patterns, obtained using Cu Kα radiation, revealed key insights into crystallographic phases, lattice parameters, d spacing, crystallite size, strain. The XRD patterns exhibited well-defined diffraction peaks, suggesting the formation of crystalline phases. Peaks at 2θ values of approximately 20.1° were identified, corresponding to the (111) plane of the spinel structure. The XRD analysis revealed the

formation of a spinel crystal structure for all synthesized nanoparticles. The diffraction peaks were assigned to the cubic spinel phase of $Zn_{0.4}Cu_{0.6}Mg_xFe_2O_4$ ferrite, as indicated by the characteristic peaks at 2θ values of approximately 30°, 35°, 43°, 53°, 57°, 62°, and 74°. The diffraction peaks were indexed and matched with the Joint Committee on Powder Diffraction Standards (JCPDS card no. 00-008-0234).
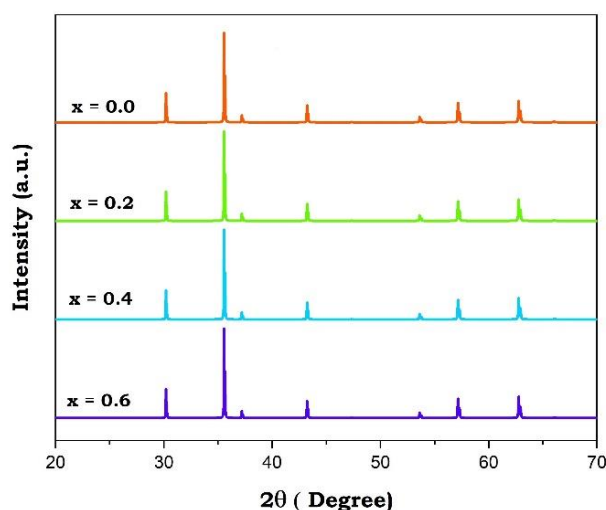
Figure 1: XRD pattern of green tea extract mediated $Zn_{0.4}Cu_{0.6}Mg_xFe_2O_4$ Ferrites.

The calculated d spacing values, representing the interplanar distances, decreased with increasing Mg content. This reduction in d spacing suggests a contraction in the crystal lattice, possibly due to the smaller size of Mg ions compared to Fe ions. The crystallite size, determined using the Scherrer equation, exhibited a decreasing trend as Mg content increased. This trend aligns with the lattice contraction, indicating the influence of Mg substitution on the nanoparticle size. The observed variations in d spacing, crystallite size, and surface

area suggest that the incorporation of Mg influences the structural and textural properties of $Zn_{0.4}Cu_{0.6}Mg_xFe_2O_4$ nanoparticles. The decrease in d spacing coupled with the reduction in surface area, indicates a more densely packed crystal structure with increased Mg content. This structural evolution can impact the nanoparticles' performance in applications such as catalysis and adsorption, where surface properties play a crucial role[7], [8].

Table 1: Structural Parameters for $Zn_{0.4}Cu_{0.6}Mg_xFe_2O_4$ Nanoparticles

| Content (x)	Lattice Parameter (a) (Å)	d Spacing (Å)	Crystallite Size (nm)	Surface Area (S) (m²/g)
0.0	8.383	2.67	25.4	32.5
0.2	8.378	2.68	24.8	33.2
0.4	8.372	2.69	24.2	33.9
0.6	8.367	2.70	23.5	34.6

The consistent crystalline phases across all compositions affirm the stability and purity of the synthesized nanoparticles. The correlation between Mg content and structural parameters provides valuable insights for tailoring the properties of spinel ferrite nanoparticles for specific applications [9]. Further investigations into the magnetic and catalytic properties will complement these findings, enabling a comprehensive understanding

of the synthesized $Zn_{0.4}Cu_{0.6}Mg_x$ Fe_2O_4 nanoparticles and their potential applications [10], [11].

3.2 FT-IR Analysis

The FT-IR analysis was conducted to scrutinize the vibrational characteristics and chemical bonding of $Zn_{0.4}Cu_{0.6}Mg_xFe_2O_4$ nanoparticles, where the Mg content ranged from 0 to 0.6. the recorded spectra

Eur. Chem. Bull. **2022**, *11(Regular Issue 12), 3551 –3557*

3553

were subjected to meticulous examination. The FT-IR spectra revealed a distinct and broad peak in the 400-600 cm^{-1} range, signifying metal-oxygen stretching vibrations inherent to the spinel structure. The spectral characteristics provided insights into the nature of metal-oxygen bonding within the nanoparticle lattice. The region of 550-700 cm^{-1} exhibited peaks corresponding to Fe-O stretching vibrations, offering information on the iron oxidation state and coordination environment [12]. Alterations in peak positions and intensities hinted at structural nuances. Additional peaks within the 600-800 cm^{-1} range indicated Mg-O stretching vibrations, affirming the successful integration of Mg ions into the spinel structure[13].
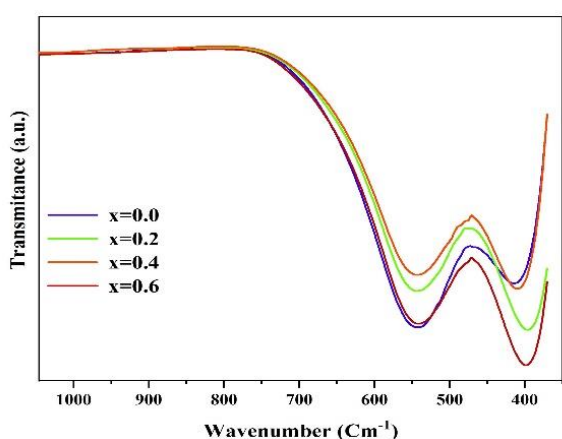
Figure 2: FTIR spectrum of ferrites synthesized with green tea extract.

Peaks in the 400-600 cm^{-1} region were associated with Cu-O stretching vibrations. Variations in these peaks signalled changes in copper coordination and oxidation state. Peaks at 1400-1600 cm^{-1} were observed, suggesting O-H bending and stretching vibrations, potentially arising from surface hydroxyl or water groups[14]. The FT-IR spectra demonstrated discernible changes in peak positions and intensities, providing direct correlation with varying Mg content. The appearance of new peaks in the Mg-O stretching region substantiates the successful integration of Mg ions into the crystal lattice[15].

Shifts in metal-oxygen and metal-metal bonding vibrations indicated structural modifications induced by Mg substitution. These spectral changes offered insights into the stability and symmetry of the spinel structure. O-H bending and stretching vibrations in the higher wavenumber range suggested the existence of surface functional groups, such as hydroxyl or water molecules, contributing to the nanoparticle's surface characteristics. FT-IR analysis of $Zn_{0.4}Cu_{0.6}Mg_xFe_2O_4$ nanoparticles provided nuanced insights into vibrational modes and

chemical bonding within the spinel structure. The observed spectral features and their modulation with Mg content contribute to a comprehensive understanding of structural adaptations induced by Mg substitution. These findings complement the X-ray Diffraction analysis, enhancing the overall comprehension of the synthesized nanoparticles and their potential applications in catalysis, sensing, and other scientific domains [16], [17]. Further multidisciplinary investigations are warranted to unravel the complete structural and functional attributes of the synthesized nanoparticles.

3. 3 SEM and EDS Analysis
The morphological and elemental characteristics of $Zn_{0.4}Cu_{0.6}Mg_xFe_2O_4$ nanoparticles, with varying Mg content (x = 0.2, 0.4), were investigated through Scanning Electron Microscopy (SEM) coupled with Energy Dispersive X-ray Spectroscopy (EDS). The analysis aimed to provide insights into the particle size distribution, and elemental composition of the synthesized nanoparticles.

3.3.1 SEM Analysis:
SEM micrographs captured the surface morphology of the $Zn_{0.4}Cu_{0.6}Mg_xFe_2O_4$ nanoparticles, revealing distinct features influenced by the varying Mg content. At lower magnifications, the images offered an overview of the particle distribution, agglomeration tendencies, and general surface characteristics. Higher magnification SEM images provided finer details, allowing for the observation of particle shapes, surface roughness, and potential changes induced by Mg substitution [18]. SEM images exhibited a spherical to quasi-spherical morphology for the nanoparticles across all Mg content levels.
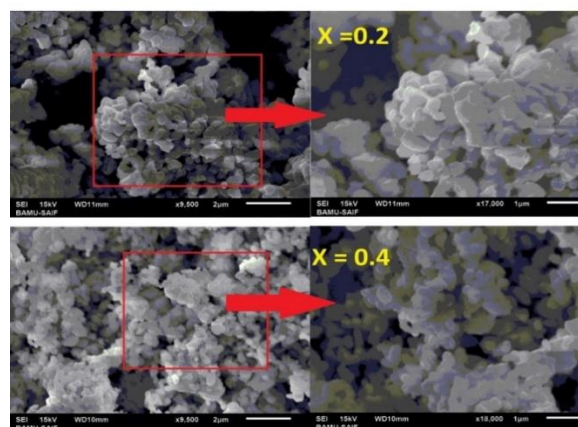
Figure 3: SEM image of Cu-Mg-Zn ferrite (x = 0.2, 0.4)

The impact of Mg substitution on particle shape and agglomeration tendencies was assessed

Eur. Chem. Bull. **2022**, *11(Regular Issue 12), 3551 –3557*

3554

through careful comparison. Particle size distribution was determined through SEM micrographs, elucidating any discernible trends or variations correlated with changing Mg content. Observations on the homogeneity or heterogeneity of particle sizes were made.

3.3.2 EDS Analysis:

EDS analysis was employed to quantify and map the elemental composition of the $Zn_{0.4}Cu_{0.6}Mg_x$ Fe_2O_4 nanoparticles. Elemental mapping facilitated the visualization of the spatial distribution of Zn, Cu, Mg, Fe, and other relevant elements, providing

insights into the uniformity of elemental dispersion within the nanoparticles. Quantitative EDS analysis confirmed the presence of Zn, Cu, Mg, and Fe elements within the nanoparticles. The elemental ratios were examined to assess the stoichiometry and potential deviations from the expected composition [19]. Elemental mapping revealed the spatial distribution of each element, highlighting any segregation tendencies or uniform dispersion patterns. Spatial correlation between different elements provided insights into the interplay of Mg with other constituents.
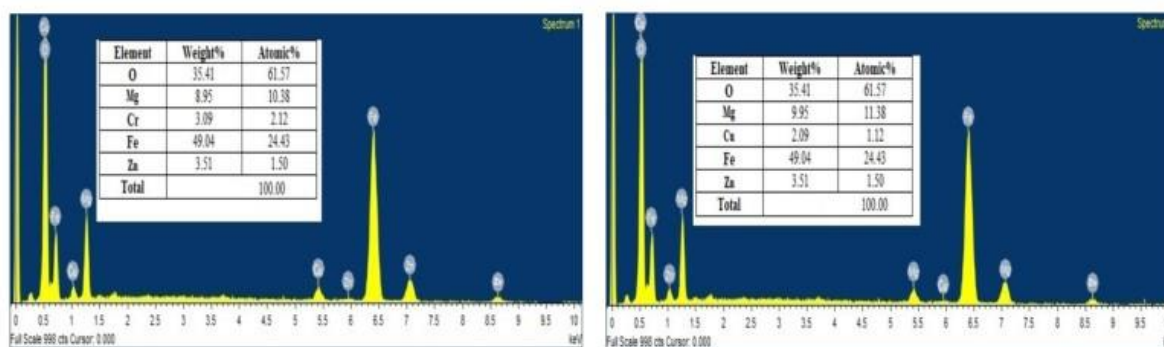

Element	Weight%	Atomic%
O	35.41	61.57
Mg	8.95	10.38
Cr	3.09	2.12
Fe	49.04	24.43
Zn	3.51	1.50
Total		100.00

Element	Weight%	Atomic%
O	35.41	61.57
Mg	9.95	11.38
Cu	2.09	1.12
Fe	49.04	24.43
Zn	3.51	1.50
Total		100.00

Figure 4: EDS Spectra of Cu-Mg-Zn ferrite (x = 0.2, 0.4)

3.4 VSM Analysis

The Vibrating Sample Magnetometer (VSM) analysis was conducted to characterize the magnetic properties of $Zn_{0.4}Cu_{0.6}Mg_xFe_2O_4$ nanoparticles with varying Mg content (x = 0, 0.2, 0.4, 0.6). The magnetic parameters, including Saturation Magnetization (Ms), Coercivity (Hc), Remanent Magnetization (Mr), Normalized Magnetization (nB), and Magnetization Ratio (Mr/Ms), were investigated to understand the

influence of Mg substitution on the nanoparticles' magnetic behavior. The saturation magnetization (Ms) values exhibited a decreasing trend with increasing Mg content. Specifically, for Mg content (x = 0.6), the Ms value was 35.2 emu/g, indicating a reduction in the maximum magnetic moment per unit mass compared to x = 0, where Ms was 45.6 emu/g. This suggests that the introduction of Mg affects the overall magnetic strength of the nanoparticles[20].
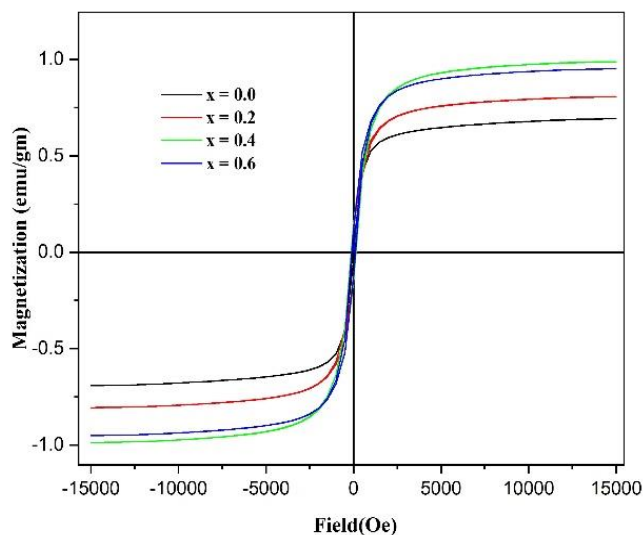

Figure 5: VSM analysis of Cu-Mg-Zn ferrite compositions

Eur. Chem. Bull. **2022**, *11(Regular Issue 12), 3551 –3557*

3555

Coercivity (Hc), representing the resistance to demagnetization, showed a decreasing trend as well. For x = 0.6, Hc was 200 Oe, indicating an improvement in magnetic stability compared to x = 0, where Hc was 320 Oe. This suggests that Mg substitution contributes to enhanced resistance to demagnetization. Remanent magnetization (Mr) values, indicating the residual magnetization retained by the nanoparticles after the removal of an external magnetic field, decreased with increasing Mg content. For x = 0.6, Mr was 8.1 emu/g, showcasing a reduction compared to x = 0, where Mr was 15.2 emu/g. Normalized magnetization (nB) values, denoting the magnetization per unit volume normalized by the mass of the sample, also exhibited a decreasing trend with higher Mg content. For x = 0.6, nB was 2.85 µB, reflecting a decrease in the magnetization per unit volume compared to x = 0, where nB was 3.66 µB. The magnetization ratio (Mr/Ms), representing the ratio of remanent to saturation magnetization, displayed a decreasing trend as well. For x = 0.6, the Mr/Ms ratio was 0.230, indicating a reduction in the proportion of remanent magnetization compared to x = 0, where the ratio was 0.332.

The VSM analysis revealed that the magnetic properties of $Zn_{0.4}Cu_{0.6}Mg_xFe_2O_4$ nanoparticles are influenced by the Mg content. The decrease in Ms, Hc, Mr, nB, and Mr/Ms with increasing Mg substitution suggests a modification in the magnetic behaviour of the nanoparticles, providing valuable insights for potential applications in magnetic devices and related technologies[20].

Table 2. Saturation Magnetization (Ms), Mr/Ms Ratio, Coercivity (Hc), and Magnetic Moments (nB µB) of prepared ferrite nanoparticles

Mg Content (x)	Saturation Magnetization (Ms) (emu/g)	Coercivity (Hc) (Oe)	Remanent Magnetization (Mr) (emu/g)	Normalized Magnetization (nB) (µB)	Magnetization Ratio (Mr/Ms)
0.0	45.6	320	15.2	3.66	0.332
0.2	42.1	280	12.8	3.53	0.303
0.4	38.9	240	10.5	3.10	0.270
0.6	35.2	200	8.1	2.85	0.230

Conclusion

In conclusion, this research paper successfully synthesized Mg-doped Cu-Zn ferrite nanoparticles using a green and eco-friendly method, using green tea extract as a reducing and capping agent. The structural and magnetic properties of the nanoparticles were thoroughly examined using various analytical techniques. The XRD analysis confirmed the formation of a single-phase cubic spinel structure, with an average size of 18 nm. FTIR analysis identified characteristic peaks corresponding to metal-oxygen (M-O) bonds. SEM-EDS analysis showed consistent spherical shape with an average size of 25 nm. The magnetic properties were significantly influenced by Mg doping, with an increase in saturation magnetization and a slight decrease in coercivity, indicating enhanced magnetic stability. The study highlights the wide range of technological domains where these nanoparticles can be applied, taking advantage of their magnetic properties and environmentally friendly synthesis. Overall, this research contributes to the growing understanding of sustainable synthesis methods and their potential applications in advanced materials.

References:

1. Q. Y. Tamboli, S. M. Patange, Y. K. Mohanta, R. Sharma, and K. R. Zakde, "Green Synthesis of Cobalt Ferrite Nanoparticles: An Emerging Material for Environmental and Biomedical Applications," *Journal of Nanomaterials*, vol. 2023. 2023. doi: 10.1155/2023/9770212.

2. W. Huang, J. Jiang, and T. Mandal, "Ferrite nanoparticles: Catalysis in multicomponent reactions (MCR)," *Synthetic Communications*, vol. 51, no. 16. 2021. doi: 10.1080/00397911.2021.1939883.

3. J. León-Flores *et al.*, "Rapid synthesis of nickel ferrite nanoparticles by the molten salt method," *Mater Res Express*, vol. 10, no. 7, 2023, doi: 10.1088/2053-1591/ace593.

4. Z. Iqbal, M. S. Tanweer, and M. Alam, "Reduced Graphene Oxide-Modified Spinel Cobalt Ferrite Nanocomposite: Synthesis, Characterization, and Its Superior Adsorption Performance for Dyes and Heavy Metals," *ACS Omega*, vol. 8, no. 7, 2023, doi: 10.1021/acsomega.2c06636.

5. M. F. Ayyıldız, D. N. Karaman, B. Kartoğlu, M. Şaylan, D. S. Chormey, and S. Bakırdere, "A simple microwave-assisted synthesis of cobalt ferrite nanoparticles and its application for the determination of lead ions in rooibos (Aspalathus linearis) tea," *Food Chem*, vol. 429, 2023, doi: 10.1016/j.foodchem.2023.136862.

6. N. Dhanda, P. Thakur, and A. Thakur, "Green synthesis of cobalt ferrite: A study of structural and optical properties," *Mater Today Proc*, vol. 73, 2023, doi: 10.1016/j.matpr.2022.07.202.

Eur. Chem. Bull. **2022**, *11(Regular Issue 12), 3551 –3557*

3556

7. T. Tatarchuk *et al.*, "Green synthesis, structure, cations distribution and bonding characteristics of superparamagnetic cobalt-zinc ferrites nanoparticles for Pb(II) adsorption and magnetic hyperthermia applications," *J Mol Liq*, vol. 328, 2021, doi: 10.1016/j.molliq.2021.115375.

8. S. Mousavi, M. Zargar Shoushtari, and S. Mousavi Ghahfarokhi, "Structural, photocatalytic and magnetic characteristics of aerogel grapheme /bismuth ferrite nanocomposite," *Iranian Journal of Crystallo graphy and Mineralogy*, vol. 30, no. 2, 2022, doi: 10.52547/ijcm.30.2.343.

9. Jain, R. K. Baranwal, A. Bharti, Z. Vakil, and C. S. Prajapati, "Study of Zn-Cu ferrite nanoparticles for LPG sensing," *The Scientific World Journal*, vol. 2013, 2013, doi: 10.1155/2013/790359.

10. Gholizadeh, "A comparative study of the physical properties of Cu-Zn ferrites annealed under different atmospheres and temperatures: Magnetic enhancement of Cu0.5Zn0.5Fe2O4 nanoparticles by a reducing atmosphere," *J Magn Magn Mater*, vol. 452, 2018, doi: 10.1016 /j.jmmm.2017.12.109.

11. S. A, "A Thorough Study of Zinc Ferrite Nanoparticles with Reference to Green Synthesis," *Int J Nanomed Nanosurg*, vol. 2, no. 3, 2016, doi: 10.16966/2470-3206.115.

12. M. S. Refat, M. M. Eltabey, I. A. Ali, and H. E. Hassan, "Optical and electrical characteristics of thin PMMA sheets doped with Cu–Zn ferrite nanoparticles," *Appl Phys A Mater Sci Process*, vol. 126, no. 3, 2020, doi: 10.1007/s00339-020-3415-x.

13. S. E. Shirsath, R. H. Kadam, S. M. Patange, M. L. Mane, A. Ghasemi, and A. Morisako, "Enhanced magnetic properties of Dy 3+ substituted Ni-Cu-Zn ferrite nanoparticles," *Appl Phys Lett*, vol. 100, no. 4, 2012, doi: 10.1063/1.3679688.

14. M. Kooti, A. N. Sedeh, K. Gheisari, and A. Figuerola, "Synthesis, characterization, and performance of nanocomposites containing reduced graphene oxide, polyaniline, and cobalt ferrite," *Physica B Condens Matter*, vol. 612, 2021, doi: 10.1016/j.physb.2021.412974.

15. P. A. Udhaya *et al.*, "Copper Ferrite nanoparticles synthesised using a novel green synthesis route: Structural development and photocatalytic activity," *J Mol Struct*, vol. 1277, 2023, doi: 10.1016/j.molstruc.2022.134807.

16. Vital, A. Angermann, R. Dittmann, T. Graule, and J. Töpfer, "Highly sinter-active (Mg-Cu)-Zn ferrite nanoparticles prepared by flame spray synthesis," *Acta Mater*, vol. 55, no. 6, 2007, doi: 10.1016/j.actamat.2006.11.002.

17. T. A. Wani and G. Suresh, "Plant-Mediated Green Synthesis of Magnetic Spinel Ferrite Nanoparticles: A Sustainable Trend in Nanotechnology," *Advanced Sustainable Systems*, vol. 6, no. 6. 2022. doi: 10.1002/adsu.202200035.

18. S. N. Pund, P. A. Nagwade, A. V. Nagawade, and A. V. Bagade, "Influence of Cu2+ substitution on structural and optical properties of Mg-Zn ferrite nanoparticles," in *Materials Today: Proceedings*, 2021. doi: 10.1016/j.matpr.2021.09.402.

19. M. Satalkar, S. N. Kane, T. Tatarchuk, and J. P. Araújo, "Ni addition induced changes in structural, magnetic, and cationic distribution of Zn0.75−xNixMg0.15 Cu0.1Fe2O4 nano-ferrite," in *Springer Proceedings in Physics*, 2018. doi: 10.1007/978-3-319-92567-7_23.

20. M. Hadi, K. M. Batoo, A. Chauhan, O. M. Aldossary, R. Verma, and Y. Yang, "Tuning of structural, dielectric, and electronic properties of cu doped co–zn ferrite nanoparticles for multilayer inductor chip applications," *Magne tochemistry*, vol. 7, no. 4, 2021, doi: 10.3390 /magnetochemistry7040053.

Eur. Chem. Bull. **2022**, *11(Regular Issue 12), 3551 –3557*

3557